Study on the local damage of SFRC with different fraction under contact blast loading

Yongliang Zhang, Kai Zhao[*], Yongchi Li, Jincai Gu, Zhongbao Ye and Jian Ma

*CAS Key Laboratory of Mechanical Behavior and Design of Materials, Department of Modern Mechanics,
University of Science and Technology of China, Hefei, Anhui 230027, China*

Abstract. The steel fiber reinforced concrete (SFRC) shows better performance under dynamic loading than conventional concrete in virtue of its good ductility. In this paper, a series of quasi-static experiments were carried out on the SFRC with volume fractions from 0 to 6%. The compressive strength increases by 38% while the tension strength increases by 106% when the fraction is 6.0%. The contact explosion tests were also performed on the $\Phi40\times6$ cm circular SFRC slabs of different volume fractions with 20 g RDX charges placed on their surfaces. The volume of spalling pit decreases rapidly with the increase of steel fiber fraction with a decline of 80% when the fraction is 6%, which is same as the crack density. Based on the experimental results, the fitting formulae are given, which can be used to predict individually the change tendencies of the blast crater volume, the spalling pit volume and the crack density in slabs with the increase of the steel fiber fraction. The new formulae of the thickness of damage region are established, whose predictions agree well with our test results and others. This is of great practical significance for experimental investigations and engineering applications.

Keywords: SFRC; blast resistant performance; spall resistant performance; damage region; blast loading

1. Introduction

Concrete is one of the engineering materials widely used in civil engineering. It is generally known that it has the brittle shortcoming because of its low tensile strength and low ductility. Thus, it is necessary to reinforce concrete by interfusing kinds of fibers with greater tensile strength and higher extension rate, in order to significantly improve the tensile strength, flexural strength and anti-blast performance (Aoude *et al*. 2015, Lee *et al*. 2014, Razaqpur *et al*. 2007). The improvement of its performance has been verified by incorporating the steel fiber, basalt fiber, polypropylene fiber, etc into the concrete (Reed *et al*. 2014, Kandasamy and Akila 2015). As SFRC is a composite material, the effective fractions of steel fiber is one of the main factors affecting the mechanical properties of SFRC (Kandasamy and Akila 2015, Shah and Ribakov 2011). At present, there is a solid foundation for the experimental research with the rapid development in SFRC technology. Perumal and Bischoff et al (Perumal 2014, Bischoff and Perry 1991) respectively studied the impact resistance and dynamic mechanical properties of SFRC by using a drop-hammer machine and SHPB. Adel Kaïkea *et al*. (2014) prepared six groups SFRC of different forms with the different fractions. The results showed that the compressive strength and peak flexural strength of the upshot concrete were strongly improved. Zhang *et al*. (2010, 2014) launched the research of the cracking rate of SFRC under different loading rate

influence, especially at low and high loading rates. However, due to the blast and impact loading, the concrete always appear spallation phenomenon on the back (Goldsmith *et al*. 1966). Sometimes there are explosion crater in front of concrete slab and spall on the back, even perforation and punch (Beppu *et al*. 2008, Almusallam *et al*. 2015). In particular, the steel fibers are currently used in civil applications to increase the anti-blast capacity of structures or to extend the structural integrity of deteriorated structures. The anti-blast and spall-resistant ability of SFRC have been recognized as an important issue in science and engineering. The blast performance of SFRC was also studied by Magnusson *et al*. (2007), and the explosive charges were placed at a stand-off distance of 10 m. The blast performance of ultra-high performance fiber-reinforced concrete was studied by Mao *et al*. (2014) with TNT placed at a stand-off distance of 7-12 m. The experimental studies about effect factor of the anti-blast performance of SFRC had been conducted with explosive charges at the stand-off distance of specimens 5 m and 0.6 m respectively by Lan *et al*. (2005), Yusof *et al*. (2011). The experimental results indicated that the specimens respectively with steel fiber of 1% and 1.5% volume fraction gave the best anti-blast performance under blast loading. But the volume fractions of steel fiber are all less than 3%, and the destruction under the contact blast loading was not paid attention. Until now, the study of the anti-blast and spall-resistant ability of SFRC under the contact blast loading is still lacking.

Moreover, there were many previous researches on impact spallation, and a series of spalling thickness formulae were put forward (Barber 1973, Jankov *et al*. 1976). But the formulae of the thickness of the damage

---

*Corresponding author, Ph.D.
 E-mail: kzhao@ustc.edu.cn, ylz001@mail.ustc.edu.cn

(a) River sand   (b) Crushed stone

(c) Steel fiber
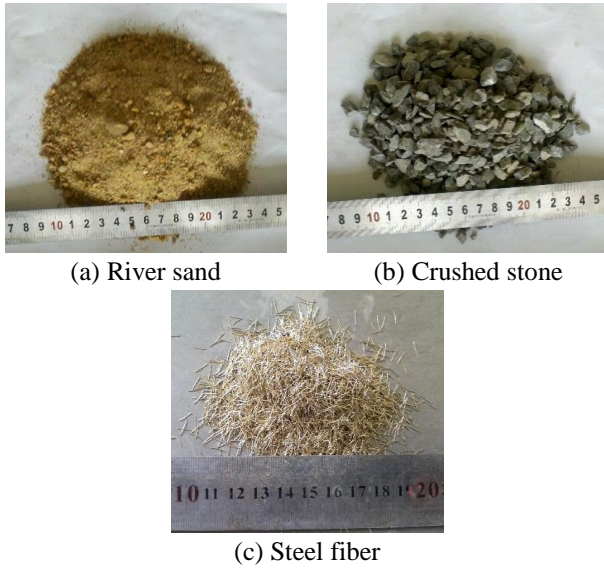
Fig. 1 Apparent shape of material

Table 1 Material properties of SFRC

Cement	P•I 42.5 Portland cement
Fine aggregate	River sand, Apparent density (dry)=2580 kg/m^3, Maximum size=5 mm
Coarse aggregate	Crushed stone, loose density(dry)=1480 kg/m^3, Maximum size=10 mm
Admixture	Fly ash, Density=2360 kg/m^3
Fiber	Steel fiber, Density=7750 kg/m^3, Diameter=0.20 mm, Length≈6.5mm
Additive	Polycarboxylate Superplasticizer

Table 2 Mixture proportions

V_f(%)	Cement (kg/m^3)	Flyash (kg/m^3)	River sand (kg/m^3)	Crushed stone (kg/m^3)
0	391.00	59.00	698.00	1090.00
0.75%	450.45	67.97	676.19	1055.95
1.50%	504.87	76.18	645.39	1007.84
3.00%	599.06	90.39	557.64	870.82
6.00%	787.43	118.82	382.15	596.76

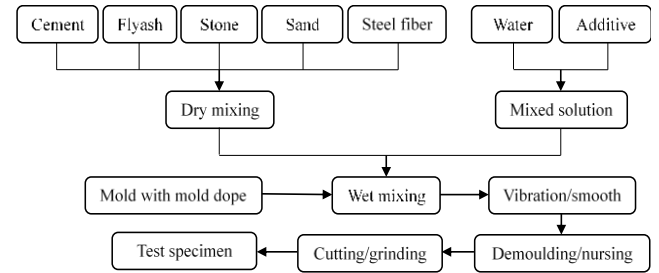Notations: V_f=Steel fiber volume Fraction; Water/(cement+flyash) ratio=0.35.

Fig. 2 Flow chart of execution processing on making specimen

region under the contact blast loading have not been reported. Only in 1989, U.S. air gave the empirical formula PCDM (Protective Construction Design Manual) about explosive spalling thickness in the handbook of protection structure design (Drake *et al.* 1989). It is noteworthy that test background of PCDM formula is TNT in the metal shell under the condition of simulated bomb, and there is a certain distance off the target. Hence, further studies are still essential in order to establish new formulae of the thickness of damage region under the contact blast loading by carrying out the contact blast tests of the SFRC with higher steel fiber fraction.

In this paper, we preliminarily focus on the effect of anti-blast and anti-spalling under the contact explosion tests. The SFRC specimens are investigated with four kinds of different steel fibers content--0.75%, 1.5%, 3.0%, and 6.0%. Based on the empiric formulae in actual application, the new formulae of the thickness of damage region under the contact blast loading are presented by combining with the basic mechanical parameters of the SFRC.

2. Materials and specimens of SFRC

2.1 Mixture proportion design

The main components of SFRC are ordinary portland cement, fly ash, river sand, crushed stone, steel fiber, water

and additive. Some of them are shown in Fig. 1. The materials employed are summarized in Table 1. The yield strength of steel fiber is 780 MPa. This size of short steel fiber was selected to avoid the fiber agglomeration in mixing process. In order to improve the bonding coefficient between cement and steel fiber, we chosed a water-cement ratio of 0.35, and the additive was 8.10 kg/m^3. The specimens of SFRC were made by the secondary synthesis method with the fiber fraction ranging from 0 to 6%. The SFRC is composed of two groups: 1) admixture cement slurry with steel fiber and 2) benchmark plain concrete, and then the mixture proportions of them were designed respectively. The mixture proportion will be eventual synthesized by accumulating components of each group. The advantage of this method is that the steel fibers were fully wrapped in the cement slurry without agglomeration. Although the steel fiber fraction is up to 6%, the fluidity is good. Mixture proportions for all specimens are shown in Table 2.

2.2 Test specimens

The dry mix composed of cement, fly ash, stone, sand and steel fibers was stirred in the first place. Secondly, the water mixed additive was into the dry mix. Then the mixture was poured into square molds, which would suffer from vibrating and smoothing. The blocks were demolded in the next day followed by being nursed in the standard nursing room for 28 days. Finally, the test specimens were made through coring, cutting and polishing. The procedure of evolution is shown in Fig. 2. Test specimens were divided into five groups with the steel fiber fraction from 0 to 6.0%. The uniaxial compression tests and Brazilian disc splitting tests were launched to obtain the quasi-static mechanical properties. The size of specimens is Φ50×100 mm in uniaxial compression test, and the size of specimens

(a) Uniaxial compression test

(b) Brazilian disc splitting test

(c) Contact explosion test
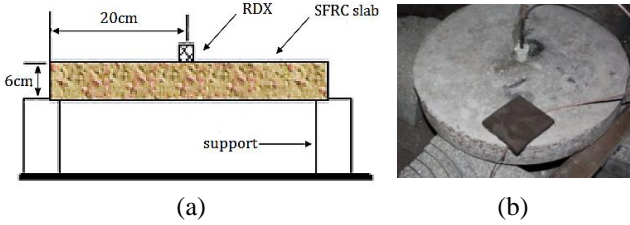
Fig. 3 Typical test specimen

(a)

(b)

Fig. 4 (a) Schematic diagram and (b) material object of experimental plan

is Φ70×30 mm in Brazilian disc splitting tests, as the specimens shown in Fig. 3(a) and Fig. 3(b).

In order to investigate the blast resistance performance of SFRC, the circular target samples were made for the contact explosion experiment. SFRC specimens were divided into four kinds of steel fiber fractions, which were 0.75%, 1.5%, 3.0% and 6.0%. The size of specimens is Φ40×6 cm, as shown in Fig. 3(c).

3. Experimental program

The uniaxial compression test and Brazilian disc splitting test were launched in Materials Test Systems by displacement control method. The loading rate of uniaxial compression test is 0.01 mm/s, and the loading rate of Brazilian disc test is 0.7 mm/s.

The contact explosion tests were performed in the laboratory of explosion mechanics and industrial safety laboratory of University of Science & Technology China. The specimens with the different fractions of steel fiber were tested, which were simply supported by rock around the block with free boundary. The cylindrical explosives used in the tests were RDX (hexogen), whose explosive heat is 5397 kJ/kg. The equivalent proportional coefficient of RDX to TNT is 1.28. The 20 g RDX was finally used for each test based on the preliminary explosion tests. The
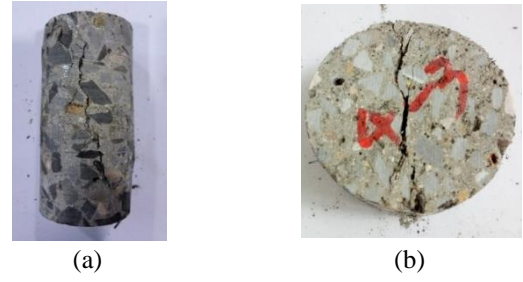

(a)

(b)

Fig. 5 The failure of SFRC specimens: (a) Uniaxial compression test, (b) Brazilian disc splitting test

Table 3 The basic mechanical parameters of SFRC

V_f (%)	f_c (MPa)	f_t (MPa)	E (GPa)
0	45.14	4.79	29.35
0.75%	55.76	5.39	30.28
1.5%	63.57	6.08	31.96
3%	71.35	7.08	32.40
6%	72.78	9.90	36.15

diameter of grain was 26 mm, high 23 mm. The RDX column was placed in the center of the surface of the specimen. The high-energy ignition device was used to set off the fuse first, and then the blast loading was loaded on the SFRC specimen, as shown in Fig. 4.

4. Experimental results

4.1 Compression and Brazilian disc splitting tensile tests results

The failure modes of uniaxial compression test and brazilian disc splitting test are shown in the Fig. 5. The compressive strength of SFRC was obtained by the uniaxial compression test. The splitting tensile strength f_t was calculated by Brazilian disc splitting test, based on the following formula Eq. (1) (ISRM 1978)

$$f_t = \frac{2F}{\pi Dh} \qquad (1)$$

where F represents the axial force, D represents the diameter of the test piece, and h represents the thickness of the specimen.

According to the uniaxial compression tests and Brazilian disc splitting tests, the basic mechanical parameters of SFRC were obtained, as shown in Table 3. It is convenient to nondimensionalize the parameters on the base of plain concrete (V_f =0%). Fig. 6 shows the histogram of these non-dimensional parameters.

As can be seen from the histogram in the diagram, the compressive strength and the splitting strength gradually increase with the increase of steel fiber fraction. The elastic modulus of SFRC substantially increases a little in virtue of the relative values in less 6% volume fraction. However, when the fraction of steel fiber is 6.0%, the splitting strength increases by 106%, which is far greater than the increase of the compressive strength by 38.0%. This
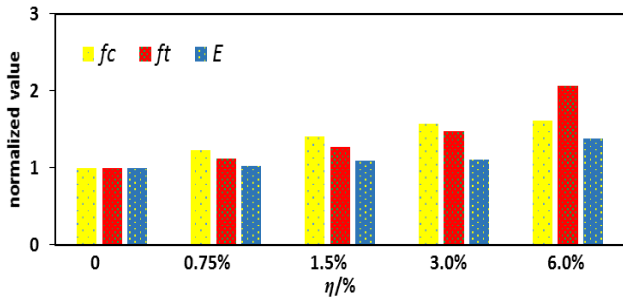
Fig. 6 The normalized value of SFRC properties with the steel fiber fraction

Fig. 7 The relationship formulae between the volume of crater and spalling pit and the content of steel fiber

illustrates that the splitting tensile strength have been improved obviously by mixing steel fibers.

4.2 Contact explosion tests results

According to the PCDM formula (Drake *et al.* 1989), it can be evaluated that the plain concrete slab must be penetrated and broken into blocks due to 20g RDX. Thus, the plain concrete (V_f=0%) was not tested. The anti-blast and spall-resistant performance of the SFRC blocks with different content from 0.75% to 6.0% were analyzed under contact explosion tests. The failure modes of the SFRC slabs are shown in Table 4.

Table 4 shows that the failure modes of cratering and spalling for each content are identical radiation expansion, but the degree of cratering and spalling differed. A crater appeared on the front surface and a spalling pit appeared on the back surface because of contact blast loading on each block. If the crater and spalling pit occurred seriously, the block would be penetrated and crushed. It was suggested that the failure modes of SFRC under contact blast loading were roughly divided into the following three types. (1) The block was thoroughly penetrated and crushed into part. (2) There were a blast crater on the surface and a spalling pit on the back surface, and the fragments had peeled off; the radial crack extended to the edge with width and depth fissures. (3) The blast crater was on the surface and a swelling with the fragments was on the back surface; the radial crack extended not to the edge with tiny and shallow fissures.
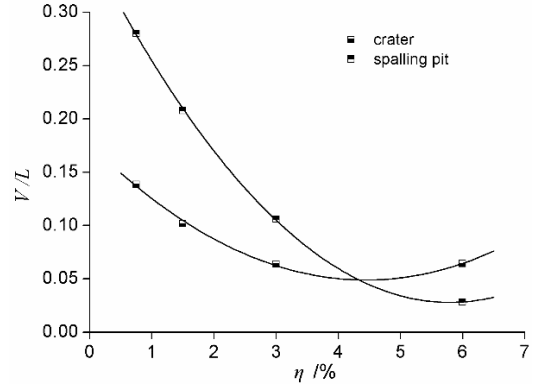
To obtain the volumes of the crater and spalling pit, they were calculated as an equivalent cone according to blasting funnel method in engineering blasting. For the case of completely penetration, we took the interface of the crater and spalling pit as the bottom, and used the vernier caliper to measure the depth of the crater and spalling pit. Then the diameters of the pithead were measured. The results of contact blast tests are shown in Table 5. The solid black line with lower half black square represents the relation between crater volume V_1 and steel fiber volume fraction η, and the solid black line with upper half black square represents the relation between spalling pit volume V_2 and η. Fig. 7 shows the comparison of the computational volume of crater and spalling pit after tests. At the same time, the fracture density μ was introduced with the help of geological concept, namely the fracture number per unit area. To acquire the relation between μ and η, the statistics were conducted about the fracture density of SFRC on the back surface, as shown in Fig. 8. The relations among the current results are given by

Crater: $V_1 = 0.1761-0.0572\eta+0.0064\eta^2$ $0<\eta<8\%$ (2)

Spalling pit: $V_2 =0.3586-0.1142\eta+0.0098\eta^2$ $0<\eta<8\%$ (3)

crack density: $\mu= 78.29-23.80\eta+2.130\eta^2$ $0<\eta<8\%$ (4)

As shown in Fig. 7, the volume of crater gradually decreases and then tends to increase with the increase of

Table 4 The failure patterns of SFRC slabs

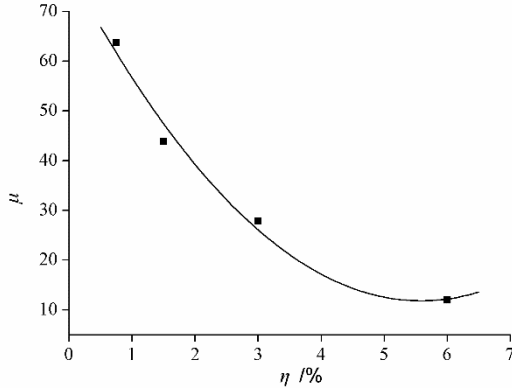| V_f (%)	0.75	1.5	3.0	6.0
front surface				
rear surface				

Fig. 8 The relationship formula between crack density and the content of steel fiber

Table 5 The results of blast tests

V_f	0.75%	1.5%	3.0%	6%
V_1 (L)	0.138	0.102	0.063	0.064
V_2 (L)	0.280	0.207	0.106	0.028
μ	63.69	43.79	27.87	11.94

steel fiber fraction. When the fraction is 3%, the volume of crater is almost cut by 60% and the volume of spalling pit gradually decreases all along with the increase of steel fiber fraction. The crack density decreases rapidly with the increase of steel fiber fraction with a decline of 80% when the fraction is 6%, which is same as the volume of spalling pit, as shown in Fig. 8. The volume V_1 of crater mainly brings out the anti-blast characteristics of the steel fiber reinforced concrete. It is summarized that the anti-blast ability increases with the increase of the fraction of steel fiber for the most part of 0~6%. The reason is that the higher the steel fiber fraction, the higher the strength and toughness of SFRC. This is consistent with the above quasi-static compression mechanical qualities and the current research achievements at low strain rates (Shah and Ribakov 2011, Wille *et al.* 2016). However, the increasing rate of anti-blast ability gradually decreases with the increase of the fraction of steel fiber. And, a slight increase of crater volume anomalously happens at near 6%. This may be brought about by the increase of the inner cavity of the SFRC because of the more inhomogeneity for higher fiber fraction during making specimen. And this problem needs further research. The spall-resistant ability is mainly reflected by the volume V_2 of spalling pit and fracture density μ of SFRC. The two qualities V_2 and μ both decrease with the increase of steel fiber fraction η. This is because that the increase of steel fiber fraction η heightens the tensile strength and toughness of SFRC, and hence enhances the spall resistant performance of the SFRC mixture. Furthermore, according Fig. 7 the decrease rate of V_2 with the increase of steel fiber fraction is greater than that of V_1. This result is similar to the following result in the former static tests: the increase of the splitting strength with steel fiber fraction is much more than that of the compressive strength. Because of the ductile fracture of SFRC, the specimens have obvious deformation or other types of damage before failure. A large number of

experimental results (Shah 1995) show that the crack propagation process of concrete materials can be divided into three distinct stages: initial crack initiation, stable expansion and instability failure. The study of dynamic fracture toughness will be developed based on double-K criterion in the future (Xu and Reinhardt 1999).

5. Discussion on the thickness of damage region

Owing to the reason known to all the PCDM formula is not suitable for damage on the structure under contact blast loading. So far, there is no suitable formula for the contact blast loading. The empirical formula (5) was given for calculating the thickness of explosion spalling by Wang (1998)

$$h = KW^{1/3} + e \qquad (5)$$

where h is the thickness of explosion spalling, K the explosion spalling coefficient, W the mass of explosive, e the distance away from the structure.

In order to establish the new formulae of the thickness of damage region, the improvement should be made based on the empirical formula. If e is seen as structural parameters, the formula can be used to calculate the destruction of the structure for contact explosion, but it is considered that the explosion spalling coefficient K is not a constant. According to the experimental study (Shah and Ribakov 2011) and our experimental data, it is not only the explosive effective charge weight but also the material parameters and mechanical properties that influence the thickness of damage region. So the explosion spalling coefficient K should be the comprehensive embodiment of these factors, and not a constant value. Based on the proportional conversion and geometrical similarity relation of the explosion, the relation formulae were deduced about the problems of explosion cavity in rock by Wang *et al.* (2005) as

$$\left. \begin{array}{l} r_c = \dfrac{0.6W^{1/3}}{\left(\rho C^2 f_c\right)^{1/9}} \\[4mm] R_d = \left(\dfrac{\rho C^2}{4 f_c}\right) r_c \end{array} \right\} \qquad (6)$$

where r_c and R_d represent the cavity radius and radius of plastically deforming region respectively, W is the mass of explosive, ρ the density of the material and C the wave velocity of the material, f_c the compressive strength.

Considering the geometrical similarity between the front plastically deforming region and the blast destruction region as shown in Fig. 9, we introduce a scale factor α, as shown in the following formula (7)

$$h_c = \alpha R_{dc} \qquad (7)$$

where h_c represents the thickness of the blast destruction region, R_{dc} is the radius of the front plastically deforming region.

Moreover, due to the effect of reflected tensile wave in rear face, it also be generalized to the spalling destruction
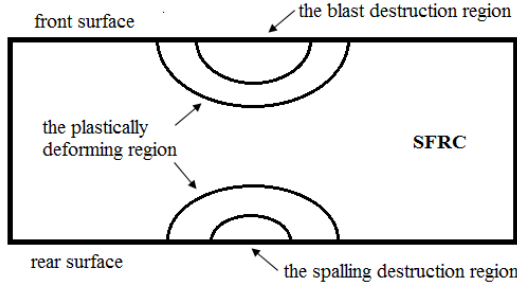
Fig. 9 The schematic diagram of plastic deformation and destruction of SFRC
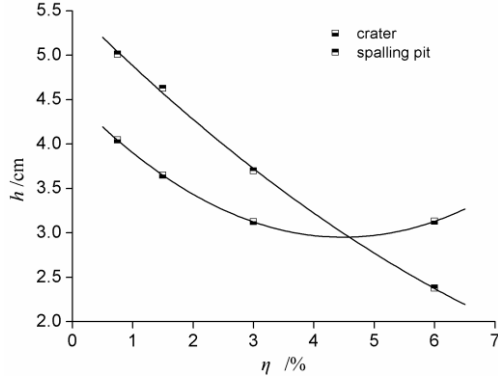

Fig. 10 The relationship between the thickness of crater and spalling pit with the content of steel fiber
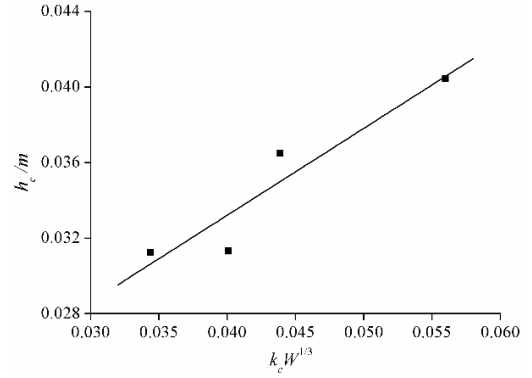

Fig. 11 The fitting results of blasting about the explosion blasting experiment
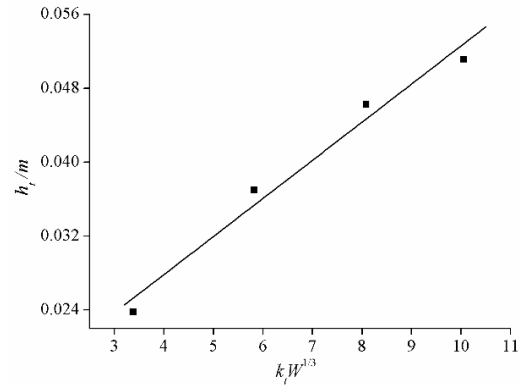
Fig. 12 The fitting results of spalling about the explosion spalling experiment

region by introducing a scale factor β, as shown in the following formula (8)

$$h_t = \beta R_{dt} \tag{8}$$

where h_t represents the thickness of the spalling destruction region, R_{dt} is the radius of the rear plastically deforming region.

To further investigate the thickness of damage region under the contact blast loading, it is acceptable to assume that the damage region is a hemisphere. According to the volume of crater and spalling pit, the thickness of damage region of the concrete target is converted into equivalent deformation thickness by using the formula (9)

$$2V = \frac{4}{3}\pi h^3 \tag{9}$$

The equivalent thicknesses of the blast destruction region and the spalling destruction region were calculated, as shown in the Fig. 10. The quadratic polynomial curve is used to fit the results and relations between the current results and fraction of steel fibers. The formulae are given by

Crater: $h_c = 4.526\text{-}0.702\eta\text{+}0.078\eta^2$ $0<\eta<8\%$ (10)

Spalling pit: $h_t = 5.673\text{-}0.762\eta\text{+}0.035\eta^2$ $0<\eta<8\%$ (11)

We tentatively put forward the below formulae (12) and (13) of the thicknesses of blasting and spalling destruction region based on the formulae (5), (6), (7) and (8).

Crater: $h_c = \alpha k_c W^{1/3} + e_c \tag{12}$

Spalling pit: $h_t = \beta k_t W^{1/3} + e_t \tag{13}$

where $k_c = \dfrac{3\rho^{8/9}C^{16/9}}{20 f_c^{20/9}} = \dfrac{3E^{8/9}}{20 f_c^{20/9}}$, $k_t = \dfrac{3\rho^{8/9}C^{16/9}}{20 f_t^{20/9}} = \dfrac{3E^{8/9}}{20 f_t^{20/9}}$

and W is the mass of explosive, ρ the density of material, C the wave velocity of the material, E the elastic modulus, f_c the compressive strength, f_t the splitting tensile strength, e_c and e_t are the structural parameters, α and β are the scale factors of blasting and spalling damage region respectively. The formulae (12) and (13) show that $h_c(h_t)$ is proportional to the $W^{1/3}$ and $k_c(k_t)$. k_c and k_t are dependent on the material parameters, which can be called the blasting and spalling failure coefficient.

The fitting results of SFRC with different steel fiber fraction of blasting and spalling are shown in Fig. 11 and Fig. 12 respectively, and the $\alpha=0.46(R^2=0.89)$ and $\beta=0.0041$ $(R^2=0.97)$ have been gained by fitting the formulae and our experimental data. The formulae can be used to predict the thickness of destruction region of SFRC under contact blast loading, and also to predict the thickness of destruction region of other materials or under other contact blast loading. Due to blasting, damaged areas in fiber-reinforced concrete (FRC) slabs were studied by Ohtsu *et al.* (2007). The equivalent deformation thickness could be calculated by Eq. (9) according to the volumes of the damaged areas. Then, the test data were analyzed and fitted by applying the preceding method Eq. (12), and it is also ideal (see Fig. 13), which gives the $\alpha=0.24(R^2=0.91)$. This shows the
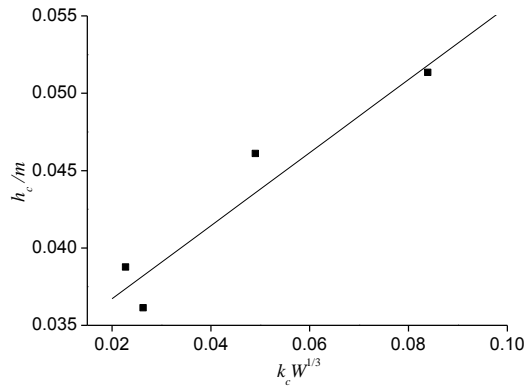
Fig. 12 The fitting results of blasting about the FRC experiment by Ohtsu *et al.* (2007)

correctness of our formulae. However, it is worth noting that we must take into account the size effect of the target and the explosive when analyzing the thickness of spalling destruction region as well as numerical simulation, which is also our next focus in the future.

6. Conclusions

The study focuses on the relation between the local damage of SFRC and the steel fiber content under the contact blast loading. The secondary synthesis method was contributed to design the mixture proportions of SFRC with the fraction of steel fibers up to 6%, and the contact blast tests were accomplished. According to the series of experiments, the changing process of compressive strength could be divided into 2 stage: the gradually increases stage and the stage tending to be stable. However, the splitting strength always increased with the increase of steel fiber fraction.

To summarize, the conclusion can be reached that the spall-resistant ability increases 80% more strikingly with the increase of steel fiber fraction than the anti-blast ability. The fitting formulae are proposed to predict individually the change tendencies of the blast crater volume, the spalling pit volume and the crack density with the increase of the steel fiber fraction.

Finally, the new formulae are established which give the dependent relations of the thickness of the blasting and spalling destruction region to the material parameters. In general, this theory provides an alternative foundation for damage analysis under the contact blast loading, and applies to other materials. The scale factors $\alpha=0.24$ were obtained by fitting the formulae to other experimental data.

This study contains some conclusions plus some ideas for further work, which have important practical implications for experimental investigations and engineering application to solve pertinent issues.

Acknowledgments

References

Almusallam, T.H., Abadel, A.A., Al-Salloum, Y.A., Siddiqui, N.A. and Abbas, H. (2015), "Effectiveness of hybrid-fibers in improving the impact resistance of RC slabs", *Int. J. Impact Eng.*, **81**, 61-73.

Aoude, H., Dagenais, F.P., Burrell, R.P. and Saatcioglu, M. (2015), "Behavior of ultra-high performance fiber reinforced concrete columns under blast loading", *Int. J. Impact Eng.*, **80**, 185-202.

Barber R.B. (1973), *Steel Rod/Concrete Slab Impact Test (Experimental Simulation)*, Bechtel Corporation.

Beppu, M., Miwa, K., Itoh, M., Katayama, M. and Ohno, T. (2008), "Damage evaluation of concrete plates by high-velocity impact", *Int. J. Impact Eng.*, **35**(12), 1419-1426.

Bischoff, P.H. and Perry, S.H. (1991), "Compressive behaviour of concrete at high strain rates", *Mater. Struct.*, **24**(6), 425-450.

Drake, J.L., Twisdale, L., Frank, R., Dass, W., Rochefort, M., Walker, R., ... and Sues, R. (1989), *Protective Construction Design Manual*, ESL-TR-87-57, Air Force Engineering and Services, Tyndall Air Force Base.

Goldsmith, W., Polivka, M. and Yang, T. (1966), "Dynamic behavior of concrete", *Exper. Mech.*, **6**(2), 65-79.

ISRM and ISRM (1978), "Suggested methods for determining tensile strength of rock materials", *Int. J. Rock Mech. Min. Sci. Geomech. Ab.*, **15**(15), 99-103.

Jankov Z.D., Shanahan, J.A. and White, M.P. (1976), "Missile tests of quarter-scale reinforced concrete barriers, A symposium on tornadoes, assessment of knowledge and implications for man", Texas Tech University, Lubbock, TX.

Kaïkea, A., Achoura, D., Duplan, F. and Rizzuti, L. (2014), "Effect of mineral admixtures and steel fiber volume contents on the behavior of high performance fiber reinforced concrete", *Mater. Des.*, **63**, 493-499.

Kandasamy, S. and Akila, P. (2015), "Experimental analysis and modeling of steel fiber reinforced scc using central composite design", *Comput. Concrete*, **15**(2), 215-229.

Lan, S., Lok, T.S. and Heng, L. (2005), "Composite structural panels subjected to explosive loading", *Constr. Build. Mater.*, **19**(5), 387-395.

Lee, D.H., Hwang, J.H., Ju, H. and Kang, S.K. (2014), "Application of direct tension force transfer model with modified fixed-angle softened-truss model to finite element analysis of steel fiber-reinforced concrete members subjected to shear", *Comput. Concrete*, **13**(1), 49-70.

Magnusson, J. and Student, P.D. (2007), "Fibre reinforced concrete beams subjected to air blast loading", *Int. J. Nordic Concrete Res.*, **35**, 18-34.

Mao, L., Barnett, S., Begg, D., Schleyer, G. and Wight, G. (2014), "Numerical simulation of ultra high performance fibre reinforced concrete panel subjected to blast loading", *Int. J. Impact Eng.*, **64**(64), 91-100.

Ohtsu, M., Uddin, F.A.K.M., Tong, W. and Murakami, K. (2007), "Dynamics of spall failure in fiber reinforced concrete due to blasting", *Constr. Build. Mater.*, **21**(3), 511-518.

Perumal, R. (2014), "Performance and modeling of high-performance steel fiber reinforced concrete under impact loads", *Comput. Concrete*, **13**(2), 255-270.

Razaqpur, A.G., Tolba, A. and Contestabile, E. (2007), "Blast loading response of reinforced concrete panels reinforced with externally bonded gfrp laminates", *Compos. Part B*, **38**(5-6),

535-546.

Reed, M., Lokuge, W. and Karunasena, W. (2014), "Fiber-reinforced geopolymer concrete with ambient curing for in situ applications", *J. Mater. Sci.*, **49**(12), 4297-4304.

Shah, A.A. and Ribakov, Y. (2011), "Recent trends in steel fibered high-strength concrete", *Mater. Des.*, **32**(8-9), 4122-4151.

Shah, S.P. (1995), *Fracture Mechanics of Concrete: Applications of Fracture Mechanics to Concrete*, Rock and Other Quasi, Wiley.

Wang, M.Y., Deng, H.J. and Qian, Q.H. (2005), "Study on problems of near cavity of penetration and explosion in rock", *Chin. J. Rock Mech. Eng.*, **11**(4), 609-616.

Wang, N.Q. (1998), *Calculation Principle and Design of Protective Structure*, PLA University of Science and Technology, Nanjing.

Wille, K., Xu, M., El-Tawil, S. and Naaman, A.E. (2016), "Dynamic impact factors of strain hardening uhp-frc under direct tensile loading at low strain rates", *Mater. Struct.*, **49**(4), 1351-1365.

Xu, S. and Reinhardt, H.W. (1999), "Determination of double- k, criterion for crack propagation in quasi-brittle fracture, part ii: analytical evaluating and practical measuring methods for three-point bending notched beams", *Int. J. Fract.*, **98**(2), 151-177.

Yusof, M.A., Norazman, N., Ariffin, A., Zain, F.M., Risby, R. and Ng, C.P. (2011), "Normal strength steel fiber reinforced concrete subjected to explosive loading", *Int. J. Sustain. Constr. Eng. Technol.*, **1**(2), 127-136.

Zhang, X.X., Ruiz, G. and Elazim, A.M.A. (2014), "Loading rate effect on crack velocities in steel fiber-reinforced concrete", *Int. J. Impact Eng.*, **76**, 60-66.

Zhang, X.X., Yu, R.C., Ruiz, G., Tarifa, M. and Camara, M.A. (2010), "Effect of loading rate on crack velocities in hsc", *Int. J. Impact Eng.*, **37**(4), 359-370.

CC